

The Thermal Contact Conductance of Hard and Soft Coat Anodized Aluminum

M. A. Lambert

Graduate Research Assistant.
Student Mem. ASME

E. E. Marotta

Graduate Research Assistant.
Student Mem. ASME

L. S. Fletcher

Thomas A. Dietz Professor.
Fellow ASME

Mechanical Engineering Department,
Texas A&M University,
College Station, TX 77843-3123

An experimental investigation of the thermal contact conductance of anodized coatings, synthesized at different bath temperatures and in different electrolyte solutions, was performed, and the results were compared with previously published information. Electrolyte solutions of sulfuric acid at bath temperatures of 7°C (Type III) and 25°C (Type II) and chromic acid at a bath temperature of 54°C (Type I) were used to grow coating thicknesses ranging from 3.2 to 61 μm (0.11 to 2.4 mil). Experimental thermal contact conductance data were obtained for a junction between anodized aluminum 6101-T6 and uncoated aluminum A356-T61 as a function of apparent contact pressure and anodized coating thickness. Apparent contact pressure ranged from 172 to 2760 kPa (25 to 400 psi) and the mean interface temperature was maintained at 40°C (104°F). The thermal contact conductance for the low-temperature sulfuric acid anodized (Type III) coatings varied from 300 to 13,000 W/m² K, while the conductance of the room temperature sulfuric acid anodized (Type II) coatings varied between 100 to 3000 W/m² K. The chromic acid (Type I) coatings yielded conductance values of 60 to 3000 W/m² K. In general, the use of elevated temperatures for the anodizing bath will lead to lower surface microhardness and lower thermal contact conductance. The greatest conductance measurements were obtained for coatings grown in low-temperature sulfuric acid.

Introduction

The thermal performance of microelectronic components has become increasingly important as systems are miniaturized. The dense packaging on standard electronic modules (SEM), widely used in military applications, often leads to thermally induced failures because of the thermal resistance occurring between the module guide ribs and the chassis card rails. This thermal resistance results from the limited contact area at the interface, the uneven contact pressure, surface characteristics, and the bulk resistance of the coatings on the card rails and guide ribs.

As circuit densities have increased, cooling schemes have been developed to maintain device temperatures within their optimum design specification. However, other techniques that help reduce the temperature change across component interfaces must also be investigated. Many electronic systems incorporate anodized surfaces, which contribute to the thermal resistance at component interfaces. This paper reports the results of an experimental investigation of anodized films grown at different temperatures and in different electrolyte solutions, and compares these results with previously published information.

Tsao and Heimburg (1970) observed that very thin oxide films on aluminum 7075-T5 resulted in only small reductions in the thermal contact conductance, while thicker oxide coatings significantly reduced the thermal conductance. Mikic and Carnasciali (1970) developed an analytical technique for predicting the thermal behavior of oxide layers. Assuming constant heat flux conditions over the contact area, the maximum discrepancy between predicted and experimental results was about 20 percent, which occurred at low layer thicknesses. Therefore, their experimental results indicated a slight increase in conductance due to thin layers. Kharitonov et al. (1974) considered the effects of oxide layers with thickness not exceeding 1 μm on the surface of metals. They concluded that the contact resistance has a weak dependence on the thermal conductivity of the oxide layer for the contact of wavy or rough surfaces.

Yip (1975) developed a prediction expression for the contact resistance of oxidized metal surfaces. His expression for estimating contact resistance includes as variables: surface roughness, asperity slope, nondimensional oxide thickness, the ratio of apparent pressure to substrate metal hardness, and the thermal conductivities of both the metal and its oxide. The theory predicts a 100-fold increase in contact resistance for aluminum with an oxide thickness approximately equal to the surface roughness.

Mian et al. (1979) examined the contact resistance of oxide films on samples of mild steel. The test specimens were lapped flat, then sandblasted to a roughness of 0.08 μm (3.2 μin.). Their data indicated that the thermal contact resistance decreased with increasing load and surface roughness. They stated that film thickness, rather than surface roughness, was the dominant variable affecting the resistance. They also demonstrated that their experimental data were in reasonably good agreement with Yip's theory.

Khan et al. (1969) conducted an experimental investigation of the thermal contact resistance of thick oxide layers synthesized on two steel alloys. The oxide films produced were light gray in color and varied in thickness from 242 to 1940 μm (0.0095 to 0.0764 in.) and exhibited a porosity in the range of 20 to 25 percent. The data indicate that break-up of the oxide layer leads to lower contact resistance only after sufficient deformation has occurred for the base metal to flow through the cracks in the oxide layer. Correlation of the data shows that at high loads the thermal contact resistance depends primarily on the oxide layer thermal conductivity and thickness, while at low pressure the oxide layer surface roughness is also important.

Al-Astrabadi et al. (1980) developed a theoretical prediction for the thermal resistance of a contact between two nominally flat randomly rough oxidized metallic surfaces. They concluded that formation of oxides tends to reduce the true metal-to-metal contact for freshly assembled joints, especially at high temperatures, thus increasing the thermal contact resistance.

Their experimental measurements consisted of six contact assemblies formed between the flat faces of 12 cylindrical specimens of EN3B mild steel. The flat faces were ground, lapped, and polished to optical flatness, and then cleaned with both acetone and isopropyl alcohol. Uniform thicknesses of oxide film, which ranged from 0.055 to 0.118 μm (2.2 to 4.6 μin.), were

Contributed by the Heat Transfer Division for publication in the JOURNAL OF HEAT TRANSFER. Manuscript received by the Heat Transfer Division November 1993; revision received May 1994. Keywords: Conduction, Electronic Equipment, Thermal Packaging. Associate Technical Editor: R. Viskanta.

grown in a high-temperature furnace and surface roughnesses varied from approximately 0.12 to 2.0 μm (4.7 to 79 $\mu\text{in.}$).

The authors assume that when the oxide layer thickness exceeds the surface roughness, the thermal contact resistance will be greater than that for the bare surfaces at all load conditions. However, if the layer thickness is of the order of or less than the surface roughness, then the thermal contact resistance would decrease only if the oxide layer hardness is less than the substrate hardness or if the oxide layer fractures. The latter mechanism would lead to greater metal-to-metal contact and lower thermal contact resistance.

Peterson and Fletcher (1990) conducted an experimental investigation to determine the thermal contact conductance and effective thermal conductivity of anodized coatings. The authors tested seven anodized aluminum 6061-T6 specimens with coating thicknesses between 60.9 and 163.8 μm (2.5 to 6.8 mils) in contact with a single bare aluminum surface. They estimated the effective thermal conductivity of the anodized coatings as the reciprocal of the slope of the overall thermal resistance as a function of coating thickness.

Keller et al. (1953) conducted an experimental investigation, using an electron microscope, of the structural features of the porous type of anodic oxide coating as synthesized on aluminum. Their investigation revealed that anodic oxide coatings consist of close-packed cells, predominantly hexagonal in shape, with each cell containing a single pore above a fully dense "barrier layer." They concluded that pore size was directly influenced by the solution electrolyte used and independent of forming voltage, while wall and barrier layer thickness are primarily functions of forming voltage.

Experimental Program

The experimental program involved the evaluation of the thermal conductance for selected anodized coatings. The test facility, test specimen characteristics, anodization process, and test procedure are all described.

Test Facility. The experimental test facility used in this investigation consists of a vertical stack consisting of a frame with sliding plates for supporting two combination heat source/sink specimen holder assemblies, the heat flux meters (specimens), a load cell, and pneumatic bellows as shown in Fig. 1. The axial force on the test column is applied by pressurizing the bellows and the contact load is monitored by a BLH load cell and signal amplifier. Uniform contact pressure over the test interfaces is assured by the use of hardened steel ball bearings to transfer load from the frame to the source-sink-holder assemblies and in turn to the specimens. Flexible neoprene hoses are used to supply coolant to the holder assemblies in order to essentially eliminate lateral loads that would skew the pressure distribution over the interfaces.

The experimental facility is housed in a vacuum chamber. A pressure of 10^{-5} torr is attained by a Varian VHS-6 oil diffusion pump backed by an Alcatel 2300 two-stage rotary pump. The vacuum pressure is monitored by thermocouple and filament gages connected to a Perkin Elmer Monitorr 300 indicator.

Test Specimens. The thermal contact conductance heat flux meters are all 2.54 cm (1.0 in.) in diameter. The upper and lower

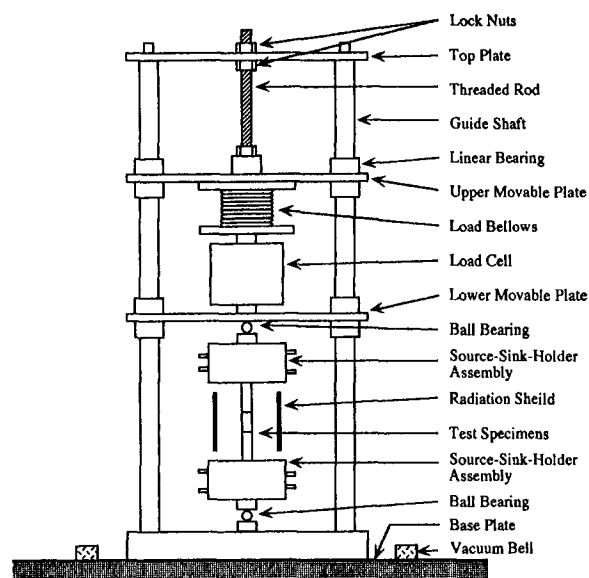


Fig. 1 Schematic of the thermal contact conductance test facility

heat flux meters are 10.16 cm (4 in.) long and are fabricated from aluminum alloy A356-T61, while the middle heat flux meter is 3.81 cm (1.5 in.) long and is machined from aluminum alloy 6101-T6. This particular alloy is used for standard electronic module frames due to its relatively high thermal conductivity (approximately 208 W/m K at 25°C as compared to 167 W/m K for the more common aluminum alloy 6061-T6). The surfaces of the aluminum 6101-T6 heat flux meters were anodized using the electrolytes and procedures described below.

Each heat flux meter was instrumented with five special limit of error (1.1°C) K type thermocouples (AWG 30) inserted into 0.12 cm (0.0465 in.) diameter holes drilled radially to their axes at 0.635 cm (0.25 in.) intervals. Aluminum powder was then tamped into the holes to ensure good thermal contact of the thermocouple beads to the peripheries of the holes. The thermocouples are connected to a Hewlett Packard 3497A data acquisition unit, which communicates with a personal computer.

Anodization Process. Three types of anodic coating were synthesized. These entailed sulfuric acid electrolyte processing at temperatures of 7°C and 25°C, and chromic acid electrolyte processing at 54°C.

The sulfuric acid process of anodization produces coatings that are colorless and transparent on aluminum. The thickness of the coating is limited, due to its relatively high solubility in the electrolyte, and thicknesses above 38.10 μm (1.5 mils) require specific techniques. The anodization conditions greatly influence the properties of this coating. The use of dilute solutions and lower temperatures favors harder, thicker coatings, while more concentrated solutions and increased temperatures and operating times produce coatings that are softer at the surface and harder throughout the rest of the film. In general, the properties of these coatings are closely tied to the rate of growth and the solvent action of the electrolyte, which not only determines the thickness of the

Nomenclature

F = flatness deviation
 h = thermal contact conductance
 H = hardness
 k = thermal conductivity
 P = apparent contact pressure
 q = heat flux through interface

R = roughness
 S = asperity slope
 t = coating thickness
 ΔT = temperature discontinuity across interface
 x = distance from contact interface

W = waviness

Subscripts and Superscripts

a = average
 q = root mean square (rms)
 $'$ = effective

coating, but also its porosity, mechanical properties, and chemical composition.

The chromic acid anodization process provides a comparatively thin but corrosion-resistant coating and is particularly suitable when rigid structures or parts with laps, joints, or crevices are to be treated. Films produced by chromic acid anodization are generally softer than sulfuric acid coatings and the traces of electrolyte remaining in crevices are noncorrosive. Some coatings produced at higher chromic acid electrolyte compositions have been shown to comply with the military salt fog specifications.

In order to determine precisely the anodic coating thickness on the aluminum 6101 specimens, a number of coating-rate trials were performed. These trials involved coating several samples for varying lengths of time in the selected electrolytes and subsequently measuring the coating thickness by microscopic examination of the cross-sections according to ASTM Test Method B487.

Surface Characteristics. Because the profiles of the contacting surfaces have a profound effect on the measured contact conductance values, all surfaces were characterized utilizing a Federal Products Surfanalyzer 4000/5000 profilometer. The surface measurements are listed in Table 1.

Surface microhardness also substantially influences contact conductance. Consequently, a number of aluminum 6101-T6 coupons were anodized by each of the three processes to thicknesses similar to those applied to the heat flux meters employed in contact conductance tests. The Vickers microhardness (VHN) of the coupons was measured for an indenter load range of 25 to 500 grams force. The range of Vickers microhardness for each coating thickness is listed in Table 1.

Test Procedure. Each test began with insertion of the selected middle anodized aluminum 6101-T6 heat flux meter between the upper and lower aluminum A356-T61 flux meters. A special alignment fixture was clamped around the column, comprised of the three heat flux meters, to ensure exact coaxial mating of the surfaces. A light load was applied, the alignment fixture then removed, and a preload pressure of 2760 kPa (400 psi) applied. This preloading, equal to the maximum contact pressure applied during subsequent conductance tests, was performed to simulate the practice of applying maximum rated torque to wedge clamps in accordance with military specifications. The bell jar was sealed over the apparatus and evacuated. Power was supplied

to the heater on one source-sink-holder assembly, and coolant was pumped through the opposite assembly.

The reported contact conductance data are for the case of heat flux passing from the anodized aluminum 6101-T6 heat flux meter to one of the bare aluminum A356-T61 heat flux meters. Conductance measurements were obtained during reloading at pressures increasing from 172 to 2760 kPa (25–400 psi). All tests were performed at a mean interface temperature of 40°C (104°F).

Data Analysis. Once the test stack temperature profile achieved a quasi-steady-state condition, which was assumed to have occurred when the mean interface temperature changed by no more than 0.3°C per hour, a data acquisition and analysis program was executed. The temperature gradients in all three heat flux meters were computed from linear least-squares regressions of their individual thermocouple readings. Their temperature-dependent conductivities were obtained from prior calibrations. The gradients and conductivities were used to calculate the heat flux through each flux meter from Fourier's law. The temperature profiles in the three heat flux meters were extrapolated to the interfaces to obtain the temperature discontinuities across the interfaces. The thermal contact conductance was computed as the quotient of the mean heat flux across the junction and the temperature discontinuity, as follows:

$$h = \frac{q}{\Delta T} \quad (1)$$

Uncertainty Analysis. Experimental uncertainties in contact conductance data arise from a number of sources, the most dominant of which is the randomness in thermocouple readings due to slight variations in their compositions. This randomness in readings exerts its greatest influence on the computed temperature gradients, which are known to an accuracy of ±7.9 percent. The uncertainty in the interfacial temperature discontinuities is ±1.0 percent. Uncertainties in the metal thermal conductivities are ±2.38 percent for the aluminum A356-T61 and ±3.14 percent for the aluminum 6101-T6. The analysis method of Kline and McClintock (1953) yields an average overall uncertainty of ±8.9 percent.

Results and Discussion

The basic properties of these anodic coatings are closely tied to the rate of growth and the solvent action of the electrolyte,

Table 1 Surface metrological data for test specimens

Specimen Number-Surface*	Anodizing Electrolyte/Temperature/Type	t (um)	Ra (um)	Rq (um)	Wa (um)	Wq (um)	F (um)	Sq	VHN (kg/mm ²)
A356-F1	Bare	0.0	0.64	0.83	0.31	0.43	7.15	0.155	100 - 128
A356-F2	"	0.0	0.65	0.84	0.43	0.52	8.15	0.160	100 - 128
A356-F4	"	0.0	0.65	0.86	0.63	0.82	10.35	0.218	100 - 128
6101-S23T	Sulfuric Acid, 15wt%	12.2	0.77	1.02	0.84	1.03	11.25	0.202	-----
6101-S24T	7 C	24.7	1.37	1.89	1.41	1.70	22.40	0.226	143 - 259
6101-S21T	Type III, Class 2	36.5	1.14	1.47	0.85	1.04	14.65	0.232	158 - 290
6101-S20T		48.6	1.20	1.60	1.35	1.59	16.75	0.212	217 - 379
6101-S19T		60.8	1.09	1.49	1.66	2.11	17.05	0.219	217 - 315
6101-S23B	Sulfuric Acid, 15wt%	7.0	0.94	1.25	1.38	1.64	14.20	0.218	76 - 299
6101-S24B	25 C	13.5	3.74	4.74	2.42	2.87	37.00	0.273	78 - 168
6101-S21B	Type II, Class 2	20.2	0.91	1.23	0.99	1.17	13.55	0.172	102 - 200
6101-S19B		27.7	0.63	0.82	1.63	1.94	13.00	0.100	78 - 140
6101-S20B		33.7	1.15	1.56	0.88	1.10	21.20	0.122	58 - 126
6101-S12T	Chromic Acid, 10wt%	3.2	0.73	0.96	1.30	1.59	12.55	0.175	84 - 211
6101-S11T	54 C	5.3	0.62	0.81	0.83	0.96	8.60	0.154	81 - 243
6101-S8T	Type I, Class 2	7.5	1.00	1.37	1.50	1.90	17.80	0.233	69 - 220
6101-S10T		10.2	1.18	1.53	1.43	1.72	16.20	0.214	70 - 106
6101-S9T		13.2	0.91	1.18	1.37	1.62	11.90	0.165	69 - 104

*Note: Type III coatings in contact with specimen A356-F2
Type II coatings in contact with specimen A356-F1
Type I coatings in contact with specimen A356-F4

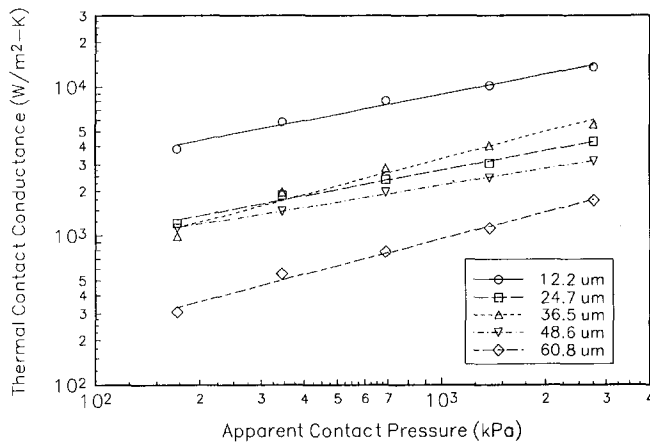


Fig. 2 Thermal contact conductance of low-temperature (7°C) sulfuric acid anodized aluminum 6101-T6 (Type III) in contact with uncoated aluminum A356 as a function of contact pressure and anodized coating thickness

which not only determines the thickness of the coating, but also its porosity, mechanical properties, and chemical composition.

The thermal contact conductance data for low-temperature (7°C) sulfuric acid anodized (Type III) aluminum 6101-T6 to bare aluminum A356-T61 are shown in Fig. 2. The thermal contact conductance varied from 300 to 13,000 W/m² K for the range of interface pressures and coating thicknesses employed. The thermal contact conductance generally decreases with increasing anodized coating thickness, and increases with increasing interface pressure.

The same trends were observed for anodized coatings synthesized using room temperature (25°C) sulfuric acid (Type II) and elevated temperature (54°C) chromic acid (Type I). The thermal contact conductance data for both 25°C sulfuric acid and chromic acid anodized coatings are shown in Figs. 3 and 4, respectively. The thermal contact conductance of the room temperature sulfuric acid anodized (Type II) coatings varied from 110 to 3000 W/m² K, while the conductance of the chromic acid anodized (Type I) coatings varied from 63 to 3000 W/m² K for the interface pressures and coating thicknesses tested.

The coatings processed at low temperature, although considerably harder than those processed at room and elevated temperature (see Table 1 for listings of Vickers microhardness), afford the greatest contact conductance, possibly because the coatings processed at low temperature are much denser, thus probably possessing higher thermal conductivity. Increasing sulfuric acid bath temperature increases electrolyte attack of the coating during growth, resulting in greater coating porosity, lower overall coating thermal conductivity, and reduced microhardness.

The Vickers microhardness (VHN) for chromic acid anodized (Type I) coatings decreases with increasing coating thickness for light indenter loads. The lower microhardness measured for thicker coatings can be attributed to enlargement of the pores as the coatings grow, due to increased electrolyte attack of the coatings with the longer processing times required to achieve greater thicknesses. The harder barrier layer, adjacent to the metallic substrate, provides higher microhardness readings for the thinner coatings. For high indenter loads the VHN for all coating thicknesses shows little variance and approximates the hardness of the aluminum 6101 substrate because the hardness of the metal dominates behavior.

The VHN for room temperature sulfuric acid anodized (Type II) coatings also showed the same general trends observed for the chromic acid anodized coatings with the highest microhardness obtained for the thinner coatings and low indenter loads.

The Vickers microhardness of low-temperature sulfuric acid anodized (Type III) coatings exhibits trends quite different from

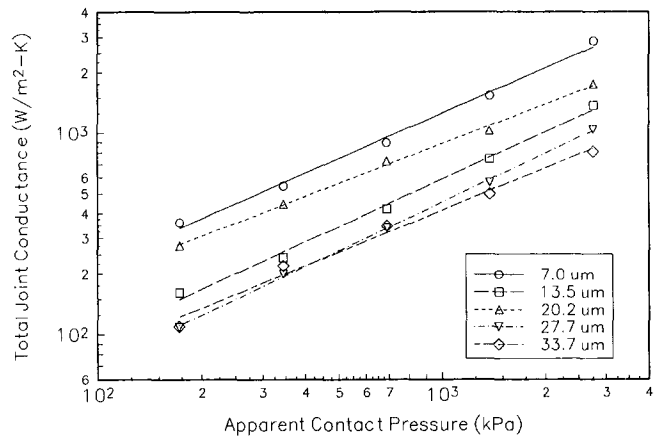


Fig. 3 Thermal contact conductance of room temperature (25°C) sulfuric acid anodized aluminum 6101-T6 (Type II) in contact with uncoated aluminum A356 as a function of contact pressure and anodized coating thickness

coating Types I and II. The microhardness of the Type III anodized coatings generally increases with increasing coating thickness and shows little dependence on load. The increase in microhardness with increasing coating thickness is due to the more uniform higher density of the coatings and the decreased influence of the aluminum substrate.

Peterson and Fletcher (1990) investigated the thermal contact conductance and thermal conductivity of several different anodized coating thicknesses. The experimental thermal conductance values of the present investigation are compared with those of Peterson and Fletcher (1990) and Lambert and Fletcher (1992) in Fig. 5. The anodizing process used by Lambert and Fletcher is the same as the 7°C sulfuric acid process used for the present investigation, while the process employed by Peterson and Fletcher was not reported. The mean junction temperature of the Lambert and Fletcher data also was the same, however, the mean junction temperature of the Peterson and Fletcher data was slightly lower (25°C). The general trend reflected by the data in Fig. 5 is that contact conductance decreases by two orders of magnitude with a factor of seven increase in coating thickness. The combined rms roughness of the contact pairs used in the present investigation and by Lambert and Fletcher (1992) is less than 2 μm, whereas the combined rms roughness reported by Peterson and Fletcher (1990) was on the order of 6 μm. All coatings were thicker than the rms surface roughness.

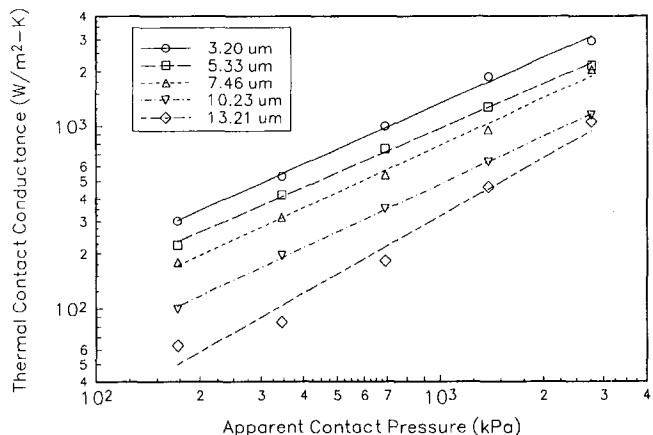


Fig. 4 Thermal contact conductance of elevated temperature (54°C) chromic acid anodized aluminum 6101-T6 (Type I) in contact with uncoated aluminum A356 as a function of contact pressure and anodized coating thickness

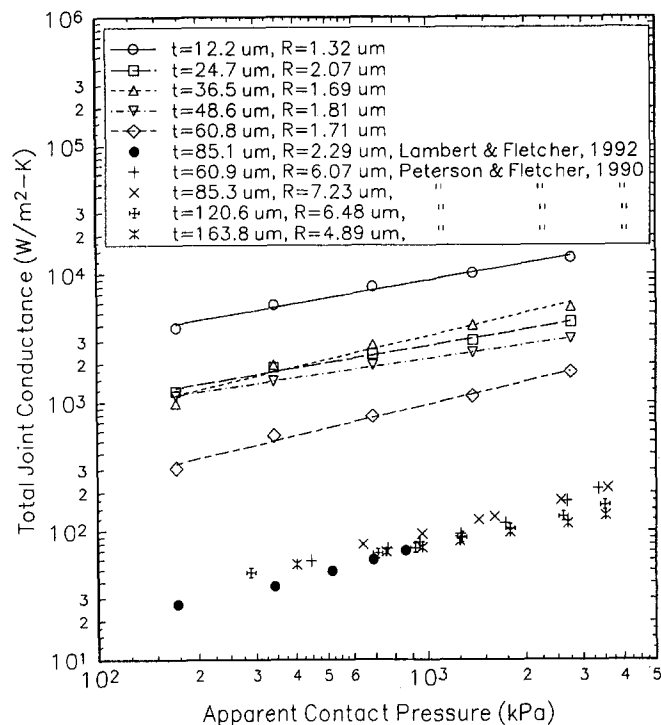


Fig. 5 Thermal contact conductance as a function of pressure and temperature for low-temperature (7°C) sulfuric acid anodized aluminum 6101-T6 (Type III) to uncoated aluminum A356-T61 with a comparison to published data

Yip (1975) and Al-Astrabadi et al. (1980) both present theories for predicting the thermal contact conductance of oxidized or anodized metals. The experimental data obtained in the present investigation, as well as data reported by Peterson and Fletcher (1990) and Lambert and Fletcher (1992), are compared to the theories of Yip (1974) and Al-Astrabadi et al. (1980) in Fig. 6. An additional theory for predicting the contact conductance of metallic coated metals, developed by Antonetti and Yovanovich (1985), is also included in Fig. 6. The dimensionless conductance and relative pressure values used in Fig. 6 were calculated using the theory of Antonetti and Yovanovich (1985), since this theory is most easily employed. The justification for using this theory for oxidized and anodized metals, originally intended for metallic coated metals, is as follows.

The theory of Al-Astrabadi et al. (1980) is analogous to a theory for metallic-coated metals developed by their colleagues, O'Callaghan et al. (1981), except that metallic coating properties in the latter theory are replaced by oxide or anodic coating properties in the theory of Al-Astrabadi et al. (1980). Lambert and Fletcher (1991) demonstrated that the theories of O'Callaghan et al. (1981) and Antonetti and Yovanovich (1985) are essentially equivalent. Therefore, the theory of Al-Astrabadi et al. (1980) closely approximates that of Antonetti and Yovanovich (1985).

As shown in Fig. 6, the dimensionless conductance values for the thick anodic coatings utilized by Peterson and Fletcher (1990) lie considerably above the theories. The results reported by Lambert and Fletcher (1992) exhibit scatter of an order of magnitude and generally fall between the uppermost theory of Al-Astrabadi et al. (1980) and the lowermost theory of Yip (1974). The conductance measurements of the present investigation are also widely scattered and somewhat evenly distributed above and below the theory of Al-Astrabadi et al. (1980).

The very high dimensionless conductance measurements for the results of Peterson and Fletcher (1990) may be due to the very low value of thermal conductivity they measured for their anodic coatings (0.0292 W/m K), in comparison to the average

thermal conductivity of six types of commercially prepared sulfuric acid anodized coatings (0.73 W/m K) as measured by Ogden et al. (1987). The conductivity value reported by Ogden et al. (1987) was used to calculate dimensionless conductance values for the results of Lambert and Fletcher (1992) and those of the present investigation. Yip (1974) assumed the thermal conductivity of the aluminum oxide films to be that of bulk aluminum oxide (32 W/m K), and Al-Astrabadi et al. (1980) assumed the conductivity of iron oxide films to be 0.875 W/m K.

Conclusions and Recommendations

This investigation presents experimental thermal contact conductance measurements for anodized coatings, synthesized at different temperatures and in different electrolyte solutions, and compares these results with previously published information and predictive theories.

The experimental data were obtained for a junction between anodized aluminum 6101-T6 and uncoated aluminum A356-T61 as a function of interface contact pressure and anodized coating thickness. The thermal contact conductance for low temperature sulfuric acid (Type III) anodized coatings varied from 300 to 13,000 W/m² K for the range of parameters tested. The lower bath temperature lowers the activity of the electrolyte as the film grows, which results in anodized coatings having higher density, higher microhardness, and higher thermal contact conductance than coating Types I and II.

The thermal contact conductance for room temperature sulfuric acid (Type II) anodized coatings varied from 110 to 3000 W/m² K, and for elevated temperature chromic acid (Type I) anodized coatings, the conductance varied from 63 to 3000 W/m² K for the range of parameters tested. Generally, the use of elevated temperatures for the anodizing bath will lead to greater electrolyte attack of the growing film during processing, resulting in greater film porosity and lower microhardness.

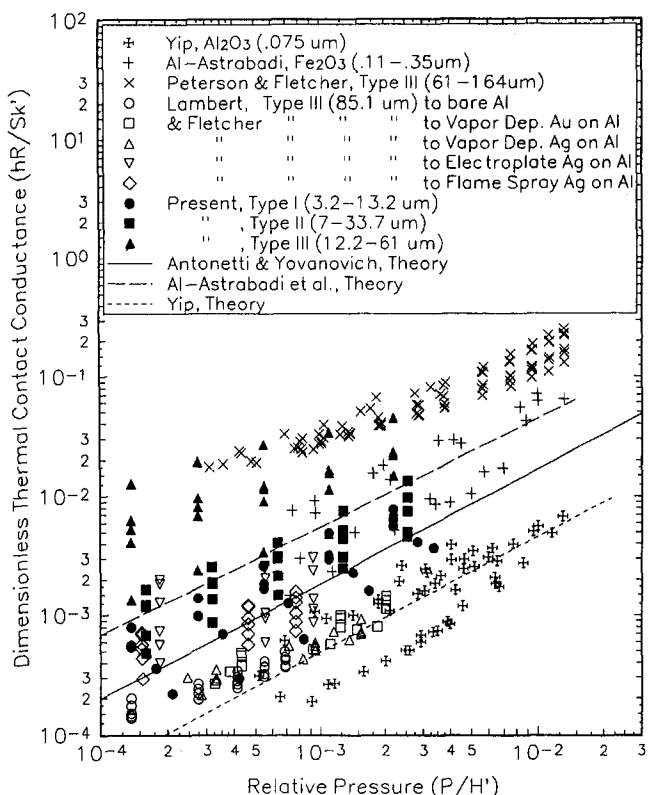


Fig. 6 Dimensionless thermal contact conductance as a function of relative pressure for oxidized steel and oxidized and anodized aluminum

The overall conductance of anodic coatings is greatly affected by coating thickness. The conductance of low-temperature (7°C) sulfuric acid anodized (Type III) coatings decreases approximately two orders of magnitude from 4000 to 13,000 W/m² K at an anodic coating thickness of 12.2 μm to 30 to 120 W/m² K at a thickness of 163.8 μm over the pressure range of 172 to 2758 kPa. The thicknesses of all coatings are greater than the average surface roughnesses of the underlying metallic substrates prior to anodization.

The theory of Al-Astrabadi et al. (1980) may overpredict or underpredict the dimensionless conductances derived from the experimental measurements of Peterson and Fletcher (1990), Lambert and Fletcher (1992), and the present investigation by as much as an order of magnitude, while the theory of Yip (1974) describes a lower bound to these data.

Acknowledgments

Support for this study was provided by NSWC Contract No. N00164-91-C-0043 and the Center for Space Power at Texas A&M University.

References

- Al-Astrabadi, F. R., O'Callaghan, P. W., and Probert, S. D., 1980, "Thermal Resistance of Contacts: Influence of Oxide Films," AIAA Paper No. 80-1467.
- Antonetti, V. W., and Yovanovich, M. M., 1985, "Enhancement of Thermal Contact Conductance by Metallic Coatings: Theory and Experiment," ASME JOURNAL OF HEAT TRANSFER, Vol. 107, pp. 513-519.
- Keller, F., Hunter, M. S., and Robinson, D. L., 1953, "Structural Features of Oxide Coatings on Aluminum," *Journal of the Electrochemical Society*, Sept., pp. 411-419.
- Khan, E. U., Dix, R. C., and Kalpakjian, S., 1969, "Thermal Contact Resistance of Thick Oxide Layers on Steel," *Journal of the Iron and Steel Institute*, Apr., pp. 457-460.
- Kharitonov, V. V., Kokorev, L. S., and Tyurin, Y. A., 1974, "Effect of Thermal Resistance," *Soviet Atomic Energy*, Vol. 36, Apr., pp. 385-387.
- Kline, S. J., and McClintock, F. A., 1953, "Describing Uncertainties in Single-Sample Experiments," *Mechanical Engineering*, Vol. 75, No. 1, Jan., pp. 3-8.
- Lambert, M. A., and Fletcher, L. S., 1991, "A Review of the Thermal Contact Conductance of Junctions With Metallic Coatings and Films," AIAA Paper No. 92-0709.
- Lambert, M. A., and Fletcher, L. S., 1992, "Metallic Coatings for Enhancing the Thermal Contact Conductance of Electronic Modules," AIAA Paper 92-2849.
- Mian, M. N., Al-Astrabadi, F. R., O'Callaghan, P. W., and Probert, S. D., 1979, "Thermal Resistance of Pressed Contacts Between Steel Surfaces: Influence of Oxide Films," *Journal of Mechanical Engineering Science*, Vol. 21, pp. 159-166.
- Mikic, B., and Carnasciali, G., 1970, "The Effect of Thermal Conductivity of Plating Material on Thermal Contact Resistance," ASME JOURNAL OF HEAT TRANSFER, Vol. 92, pp. 475-482.
- O'Callaghan, W., Snaith, B., Probert, S. D., and Al-Astrabadi, F. R., 1981, "Prediction of Optimal Interfacial Filler Thickness for Minimum Thermal Contact Resistance," AIAA Paper No. 81-1166.
- Ogden, T. R., Rathsam, A. D., and Gilchrist, J. T., 1987, "Thermal Conductivity of Thick Anodic Oxide Coatings on Aluminum," *Materials Letters*, Vol. 5, No. 3, Elsevier Science Publishers, pp. 84-87.
- Peterson, G. P., and Fletcher, L. S., 1990, "Measurement of the Thermal Contact Conductance and Thermal Conductivity of Anodized Aluminum Coatings," ASME JOURNAL OF HEAT TRANSFER, Vol. 112, pp. 579-585.
- Tsao, Y. H., and Heimbarg, R. W., 1970, "Effect of Surface Films on Thermal Contact Conductance: Part 2—Macroscopic Experiments," ASME Paper No. 70-HT-SpT-27.
- Yip, F. C., 1975, "Effects of Oxide Films on Thermal Contact Resistance," *AIAA Progress in Astronautics and Aeronautics: Heat Transfer With Thermal Control Applications*, Vol. 39, M. M. Yovanovich, ed., MIT Press, Cambridge, MA, pp. 45-46.